Optics & Laser Technology 68 (2015) 105–112

Contents lists available at ScienceDirect

Optics & Laser Technology

journal homepage: www.elsevier.com/locate/optlastec

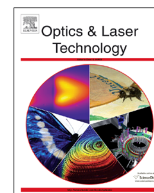

Lithographically tuned one dimensional polymeric photonic crystal arrays

D. Chavelas [a,b], P. Oikonomou [a], A. Botsialas [a], P. Argitis [a], N. Papanikolaou [a], D. Goustouridis [c], K. Beltsios [b], E. Lidorikis [b], I. Raptis [a,*], M. Chatzichristidi [a,d]

[a] Institute of Microelectronics, NCSR "Demokritos" Athens, Greece
[b] Department of Materials Science and Engineering, University of Ioannina, Ioannina, Greece
[c] Department of Electronics, TEI of Peiraeus, Egaleo, Greece
[d] Industrial Chemistry Laboratory, Department of Chemistry, University of Athens, Athens, Greece

ARTICLE INFO

Article history:
Received 21 July 2014
Received in revised form
8 October 2014
Accepted 10 November 2014
Available online 5 December 2014

Keywords:
1-D photonic crystal array
Lithography
Polymer material

ABSTRACT

One-dimensional polymeric photonic crystal (PC) arrays with tuned bandgap properties are designed and fabricated on the same substrate by employing mainstream micropatterning technologies and appropriate photopatternable materials. The two photopatternable materials are based on poly (2-hydroxy ethyl methacrylate) and epoxy polymers with the addition of appropriate photoacid generators and are diluted in orthogonal solvents, ethyl lactate and PGMEA respectively. The tuning of the photonic band gap of each photonic crystal is achieved through carefully tuned lithographic processing conditions with emphasis in low-lithographic contrast operation and gray scale lithography. By applying sequential lithographic steps in orthogonal developers one-dimensional photonic crystal arrays with 10 bi-layers are fabricated with very well defined patterns. With this approach, PC arrays with four distinct areas are realized on the same Si substrate with tuned reflectance spectrum covering the whole visible spectral regime.

© 2014 Elsevier Ltd. All rights reserved.

1. Introduction

One-dimensional (1-D) photonic crystals are sequential layers of materials with a refractive index contrast. This periodic variation of the refractive index along with thickness uniformity of each of the materials form a device with tuned reflectance properties that can be useful in a wide range of diverse applications such as solar cells, sensors, etc.

1-D Photonic Crystals (1-D PCs) have been successfully fabricated with various materials and deposition techniques. In the majority of applications dielectric layers are used, such as SiO_2, TiO_2 for devices operating in the visible range [e.g. [1,2,3]] or Si, SiO_2 for devices operating in the near infrared part of the spectrum [e.g. [4]]. In all those cases the layers present very high uniformity in thickness versus layer number. Depending on the refractive index contrast, the band gap can be wide, in case the refractive index contrast is high, or narrow in the opposite case. Due to the employed deposition methodologies, these structures are of very high quality and the spectral characteristics can be easily tuned through the refractive index contrast and the thickness of the layers (d_A, d_B). In addition sol–gel technology has been also successfully used for the realization of such structures for optical sensing applications [e.g. [5]].

Another approach that has attracted the interest of the research community is the use of polymeric materials that are applied on the substrate via spin-coating. This is a low-cost 1-D PC fabrication approach; yet (a) the materials should be selected from a small pool of polymeric materials and (b) the refractive index contrast that is achieved is small due to the limited refractive index range of polymers [e.g. [6,7,8]]. Polymeric 1-D PCs have been widely used as spectroscopic and colorimetric sensors of various analytes either in air (humidity) or in liquids that induce swelling of the employed polymeric materials; i.e., the polymeric layers are forming the PC but at the same time are sensing the layers also [e.g. [9]]. In certain cases hybrid organic/inorganic one-dimensional photonic crystals [e.g. [10]] have been developed by spin-coating and applied in the detection of organic solvents through spectral shift.

All approaches that have been proposed and applied so far proved to be reliable and can deliver 1-D PCs of very high quality and with tuned bandgap properties. However none of these technologies in their present form is able to realize 1-D photonic

* Corresponding author. Tel.: +30 2106503265; fax: +30 2106511723.
E-mail address: raptis@imel.demokritos.gr (I. Raptis).

http://dx.doi.org/10.1016/j.optlastec.2014.11.008
0030-3992/© 2014 Elsevier Ltd. All rights reserved.

crystal arrays on the same substrate with different tuned optical properties.

In order to overcome this limitation, a methodology for the realization of 1-D polymeric PC arrays is introduced and optimized in the present work. In particular, carefully selected patternable materials are applied via spin coating and each layer is processed via mainstream lithographic steps (Post Apply Bake (PAB), Exposure, Post Exposure Bake (PEB) and development). Through this sequence of lithographic processing steps, 1-D polymeric PC structures are realized. The shape and the dimensions of each PC in the array are defined through the lithographic mask and the lateral dimensions can be as small as few tens of micrometer. The photoresist formulations and the processing conditions applied in this technology have been carefully optimized in order to allow for the definition, during a single lithographic step, of patterns exhibiting the desirable variation in thickness (gray scale lithography). Due to the particular photopatternable materials used, the tuning of the thickness is possible for the two polymers independently, allowing for the realization of 1-D PC arrays e.g. as filters on top of already fabricated electronic devices. In addition the process could be also applied on flexible or transparent substrates.

2. Materials and methods

2.1. Materials

For the realization of the one dimensional polymeric photonic crystal arrays, the materials to be employed should fulfill a number of strict and diverse requirements. In particular, apart from having sufficient refractive index contrast, both materials should be patternable, the application and processing of each layer should not affect the existing layer, and the remaining layer thickness should be controllable through careful tuning of the exposure conditions. The materials selected for the fabrication of the photonic crystal arrays are poly(2-hydroxy ethyl methacrylate) (PHEMA) [e.g. [11,12]] and an epoxy based resist (EPR) [13,14]. PHEMA due to the presence of hydroxyl groups is hydrophilic while EPR is hydrophobic. Due to the high difference of hydrophilicity properties between PHEMA and EPR, this set of materials proved to be appropriate for the realization of 1-D photonic crystals for the spectroscopic monitoring of humidity levels in the environment [9].

PHEMA was purchased from Sigma-Aldrich [Mw=300000] and was diluted in ethyl lactate (EL) with or without the addition of a PhotoAcid Genarator (PAG) to form the solution for the spin coating. When PAG is added in the solution, PHEMA-N, the material operates as negative tone chemically amplified photoresist when irradiated in DUV, due to etherification and transesterification reactions that occur during heating in the presence of acid [12], Cross-PHEMA. The PAG used in PHEMA-N was triphenylsulfonium hexafluoroantimonate (TPS).

EPR was used in a PGMEA solution containing the same PAG as above (TPS) in order to render the polymer to a chemically amplified negative tone photoresist. EPR is an epoxy novolac polymer that upon photoactivation of TPS and subsequent thermal heating, a cationic chain growth polymerization occurs which takes place by ring opening polymerization of the epoxy ring, leading to a high crosslinked film, Cross-EPR [13].

The polymeric layers were applied via spin-coating (Headway Research EC101) and the thermal processing was performed on SMT150 Bioline Scientific hot-plates.

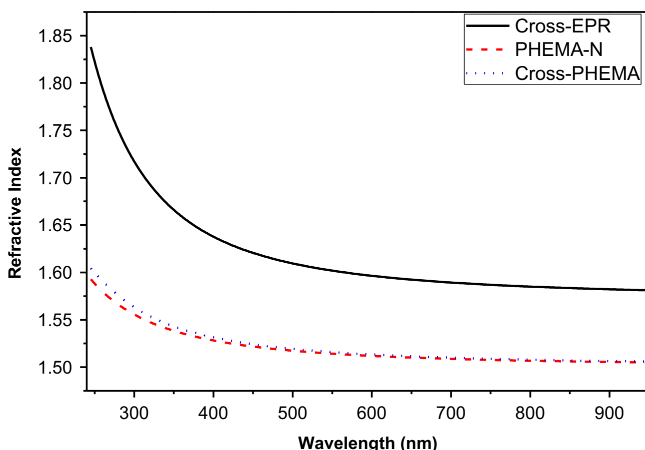

Fig. 1. Measured refractive index versus wavelength for Cross-EPR, PHEMA-N and Cross-PHEMA films. PHEMA has very small absorbance in the spectral range >280 nm [12]. This is also the case for the EPR where the absorbance for the spectral range >300 nm is practically zero [15]. Furthermore, for both materials changes in the absorption spectrum upon exposure are negligible at wavelengths >280 nm.

2.2. Materials characterization

For the realization of a photonic crystal, the two materials employed should present refractive index contrast the value of which defines at a high extent the optical properties of the photonic device. The refractive indices versus the wavelength for the materials employed in the PCs as measured with a spectroscopic ellipsometer (M2000-F, J.A. Woolam Inc.) are illustrated in Fig. 1. The refractive indices are for (a) crosslinked EPR (Cross-EPR) areas i.e. EPR areas that have been exposed at high dose and then PEB was made, (b) for PHEMA and (c) crosslinked PHEMA (Cross-PHEMA) areas i.e. PHEMA-N areas that have been exposed at high dose and then PEB was made. The refractive index of Cross-EPR is 1.59, of PHEMA is 1.51, and of Cross-PHEMA is 1.51 at 632 nm. This refractive index contrast between Cross-EPR and PHEMA layers is high enough for the fabrication of a 1-D photonic crystal with narrow band-gap width.

The optical properties of the various 1-D PC arrays were recorded with an FR-Basic tool (ThetaMetrisis) operating in reflectance mode.

2.3. Developers and solvents

In order to fabricate a high quality PC, the interfaces of the various sequential layers should be sharp. Therefore, in the case of polymeric films where spin coating is used for the application of the layers, it is critical that the solvent in the solution of each polymer does not affect the polymeric film already deposited on the substrate; this is the case of the so-called orthogonal solvents. For PHEMA-EPR photonic crystals, the solvent in the EPR solution (PGMEA) should not affect the PHEMA or cross-PHEMA layers while the casting solvents in the PHEMA solutions (EL) should not affect the Cross-EPR layer. In a previous work [9], it was shown that this prerequisite is fulfilled for the particular combinations of these polymeric materials and their solutions and 1-D PCs can be realized through sequential spin coating of those polymeric layers.

3. Results

3.1. Optimization of processing conditions

Our goal is the simultaneous fabrication of 1-D polymeric PC arrays with regions having different optical responses on the same

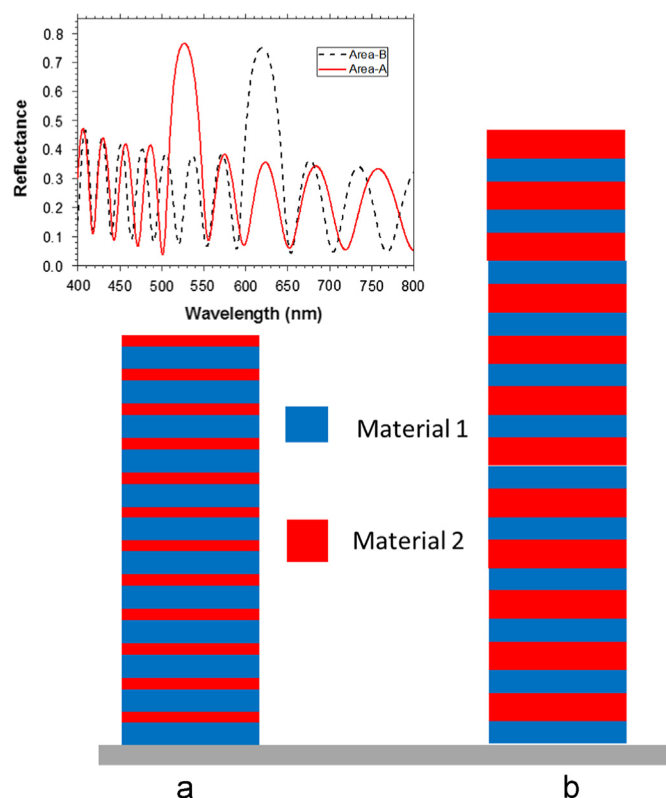

Fig. 2. One-dimensional Photonic Crystal Array on the same substrate. The different thicknesses in material-2 in the two areas causes different bandgap properties (inset) as illustrated in figure's inset. The data illustrated in the inset are for 12 bilayers of PHEMA (blue color) and cross-EPR (red color) with different thicknesses for Cross-EPR in Area-A (70 nm) and Area-B (100 nm). The thickness of PHEMA (Material-1) is 100 nm. (For interpretation of the references to color in this figure legend, the reader is referred to the web version of this article.)

patterned substrate using a sequence of spin-coating steps which to our knowledge has not been presented so far in the literature. Different bandgaps can be easy engineared by polymeric layers with different thicknesses should be deposited in each area of the array. The dependence of the optical properties on the thickness is presented in Fig. 2. In the case of photoresist films, the remaining film thickness, after a lithographic step, depends on the processing conditions i.e. the exposure dose, the PEB temperature and time and the developer. Since the 1-D PC array is realized on one substrate, the PEB and developer conditions for all PCs are the same and the film thickness modulation could be produced through exposure dose modulation only (gray scale lithography).

In order to evaluate the effect of the exposure dose on the remaining thickness after development, the contrast curves of EPR and PHEMA-N at 254 nm are illustrated in Fig. 3a and b respectively. In both cases, the effect of developer and PEB conditions was studied in terms of lithographic contrast values and the thickness modulation capabilities in the real application and the optimized conditions were determined. The lithographic contrast (γ) is one of the critical parameters for the evaluation of the lithographic performance of a photopatternable material. The lithographic contrast is usually calculated from the slope of the linear part of the normalized remaining thickness versus dose in logarithmic scale [16]. The lithographic contrast value (γ) is of high importance for the particular application since low contrast-lithographic conditions are required for the definition of the PC areas. EPR solution with 0.5% w/w PAG was spin-coated at 1000 rpm giving a film thickness of 115 nm. PAB was made at 110 °C for 5 min and then exposed at 254 nm for a wide range of exposure doses. The PEB conditions studied were 90 °C for 2 min and 110 °C for 2 min and two developers evaluated: PGMEA and MIBK for 3 min. EPR with this PAG concentration is reacting as a gray tone material having a contrast of 2.8 as seen in Fig. 3. PEB temperature of 90 °C for 2 min and MIBK as developer were chosen for the fabrication of the photonic crystal because it has the same contrast but higher quality films after development.

PHEMA was spin-coated from a 6% w/w solution in EL at 7000 rpm giving a film thickness of 140 nm and PAB was made at 120 °C for 5 min. On the other hand, when PHEMA-N was employed for the thickness modulation of both polymeric materials, it was spin-coated from a 6% w/w solution in EL with 2% w/w with respect to the polymer concentration PAG, at 7000 rpm giving a film thickness of 140 nm. PHEMA-N is also reacting as a gray tone material, especially at low exposure doses, and thus giving the capability, similar to EPR, to choose the desired thickness of the film after exposure and development, this is quantified in Fig. 3b. After the spin-coating of PHEMA-N and PAB at 120 °C for 5 min, the films were exposed at 254 nm light. PEB was set to 90 °C for 2 min with subsequent development in methanol for 1 min.

3.2. Photonic crystal fabrication

Deposition of alternating layers of PHEMA and Cross-EPR on a substrate [9] produces a PC. The first bilayer is fabricated as follows: a PHEMA film is spin-coated on the substrate and PAB follows; then an EPR film is deposited on the PHEMA layer and PAB was made, then it was exposed at 254 nm and PEB followed. The latter procedure is applied several times for the realization of the photonic crystal with the desired optical properties.

The central reflectance wavelength of PCs could be in principle any wavelength falling within a very broad spectral range starting from approximately 240 nm. The minimum wavelength of 240 nm is calculated by considering 40 nm to be the minimum polymeric layer thickness attainable at very high quality by spin coating. Furthermore, the absorbance of the selected polymers becomes high at shorter wavelengths. This way, dense arrays of PCs of any shape and with lateral dimensions down to few tens of a micron and with designed optical performance could be fabricated on the same substrate by employing standard lithographic processes. Therefore those PCs could be easily and at low-cost fabricated on top of integrated circuits at wafer-level scale by employing mainstream silicon processing equipment and add unique spatial optical filtering capabilities.

The PC array could be fabricated either by applying gray scale lithography to one or both polymeric materials employed. In our approach with the use of gray scale lithography for one of the materials, different exposure doses are applied on the EPR layers allowing for different thicknesses across the sample, whereas PHEMA layer thickness was kept constant. By applying this concept, 1-D PCs accommodating 4 different PC's were fabricated. The procedure followed for the realization of a PHEMA/Cross-EPR bilayer is illustrated in Fig. 4.

First the PHEMA film, without PAG, was applied from a 3% w/w solution via spin-coating at 3000 rpm giving a film thickness of 90nm followed by PAB at 120 °C for 5 min. Then, EPR solution 5% w/w in PGMEA with 2% PAG with respect to the polymer concentration was spin-coated on top of the PHEMA film and PAB was made at 110 °C for 5 min in order to remove the excess solvent. Exposure of the four areas with different exposure doses, 6, 8, 10 and 15×10^{-4} mJ/cm^2, was made using an appropriate mask. Exposure was followed by PEB at 90 °C for 2 min and development in MIBK for 3 min revealing 4 areas (A, B, C and D) in the substrate having different EPR thicknesses (A thinner to D thicker) and between those areas (unexposed EPR) only PHEMA film was remained from the first PHEMA layer. Then, PHEMA was

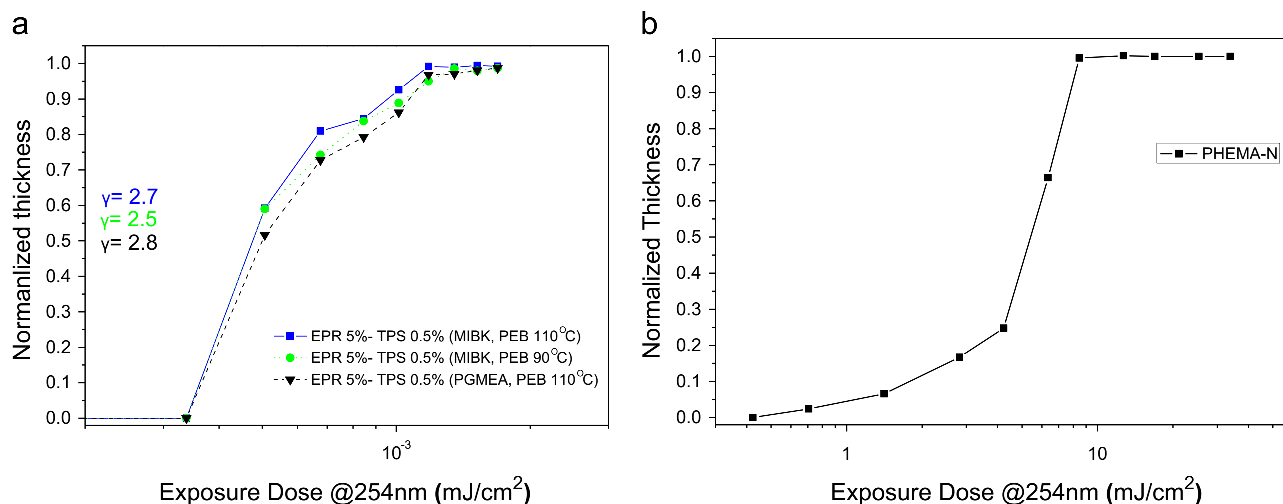

Fig. 3. Contrast curves of (a) 5%w/w solution of EPR in PGMEA with 0.5%w/w PAG, the values for γ shown in the figure are calculated from the linear part of the curve at low exposure doses and (b) 6%w/w solution of PHEMA-N in EL with 2%w/w PAG.

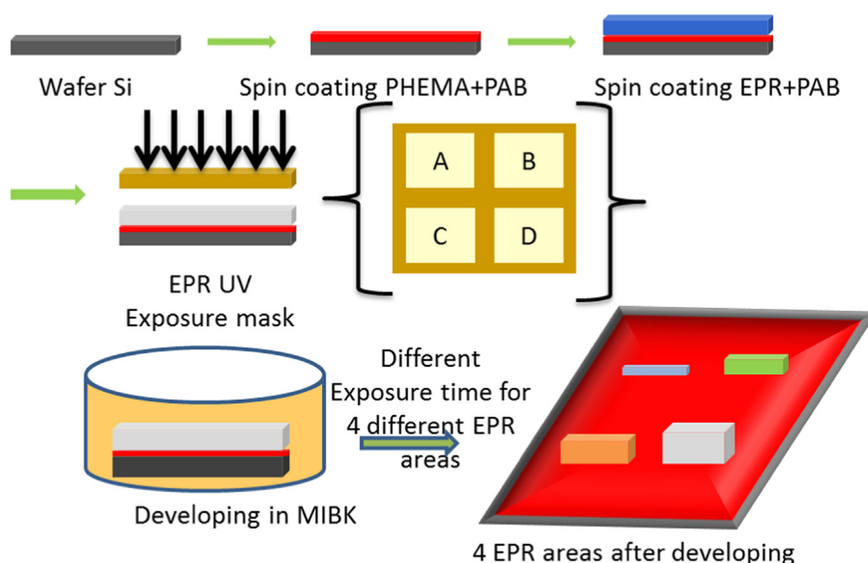

Fig. 4. Schematic presentation of the fabrication of a PHEMA/Cross-EPR array having 4 different PCs. In this scheme only the EPR acts as a lithographic material.

spin-coated on top of the patterned EPR film followed by PAB, and EPR deposition and PAB. The procedure was repeated and the same areas were exposed with the same doses etc. This way 8 bilayers of PHEMA and EPR were fabricated on the same substrate each of them having the same PHEMA thickness and different EPR thicknesses giving 4 PCs with discrete reflectance spectra. In Table 1 the average thickness of PHEMA and EPR layers for each PC is given and in Fig. 5 the layer thickness of each PHEMA and EPR film in area D (highest exposure dose) is presented as well as a cross-section SEM picture of that area. The film thickness difference of PHEMA of each PC is no more than 11%. EPR layer thickness difference for each PC is higher mostly at the lower exposure dose areas. This conclusion also arises from the fact that in the high exposure dose area (area D) the layer thickness difference was only 7%.

The reflectance spectra of all four 1-D PC areas are presented in Fig. 6a. In Fig. 6b an optical photograph of the fabricated device is shown. The bandgaps are centered from 451 nm for area-A to 554 nm for area-D covering a 100 nm spectral range. This range can be tuned by adjusting properly the processing conditions of EPR layer. E.g. by employing a wider exposure dose range this range can be increased. Generally, random variations in the layer thicknesses can have a detrimental effect on the reflectance properties of periodic multilayers. In the case of large refractive index contrast between the two materials, partial waves are strongly reflected and thus only few of those are required to build up strong total reflection. In other words, only the very few first bilayers are probed by the incident wave, and any disorder in thicknesses here is detrimental. However, this effect is

Table 1
The exposure dose for each EPR area and the average thickness and the related standard deviations of PHEMA and EPR layers for each PC of the array.

	EPR exposure dose (mJ/cm^2)	Average PHEMA thickness (nm)	Average EPR thickness (nm)
Area A	6×10^{-4}	80.2 ± 8.5	62.5 ± 14.7
Area B	8×10^{-4}	72.9 ± 8.3	82.2 ± 15.3
Area C	10×10^{-4}	70.4 ± 5.8	94.1 ± 10.7
Area D	15×10^{-4}	63.9 ± 4.8	113.9 ± 8.0

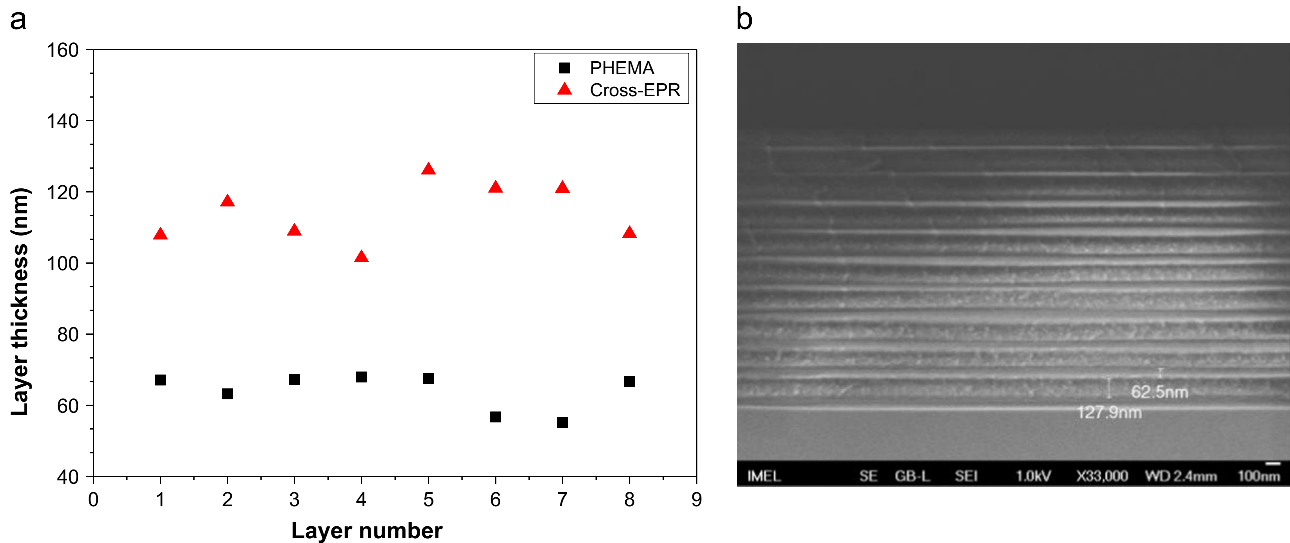

Fig. 5. (a) The layer thickness of each PHEMA and Cross-EPR film in area D (highest exposure dose) and (b) a cross-section SEM picture of that area.

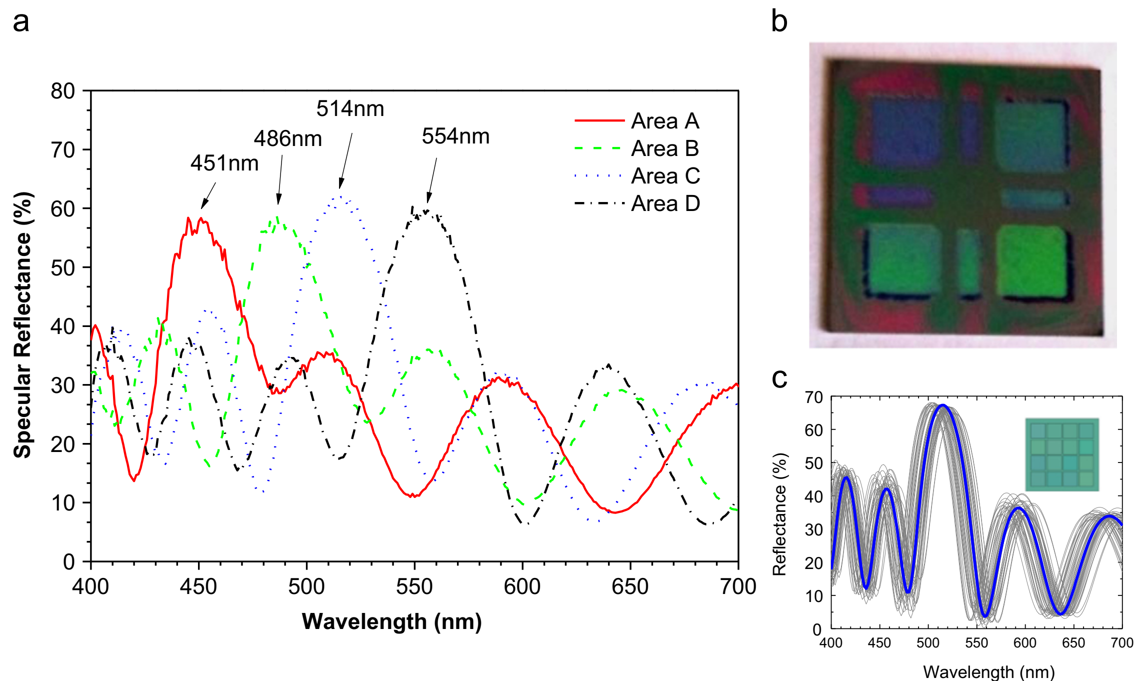

Fig. 6. (a) The reflectance spectra of each area of the PC array fabricated with the procedure described in Fig. 4. The reflectance peaks range from 451 nm (Area-A) to 554 nm (Area-D). (b) An optical image of the array. The Area-A is the top-left and the Area-D the bottom right (c) Numerical calculation of the specular reflectance for random versions of Area C using the thicknesses and standard deviations quoted in Table 1. Fifty different random realizations are shown with gray lines, while the perfect case is shown with the thick blue line. In the inset, the theoretical color of 16 different realizations is shown in the small squares, while the perfect case is shown in the large background square. (For interpretation of the references to color in this figure legend, the reader is referred to the web version of this article.)

significantly smaller when the refractive index contrast between the two materials is small. In this case, each partial wave is weakly reflected, and many multiply reflected waves must interfere to create a strong overall reflection. This means that the incident wave probes the PC into larger depths, i.e. many bilayers contribute to the reflection and the small phase differences between the multiple waves caused by disorder tend to cancel each other resulting into a sustained strong total reflection. This is quantified in our case in Fig. 6c where we show the simulated reflectance spectra variation for several multilayers with random thicknesses but within the measured standard deviation. The simulation shows that a peak reflectance variation of ~20 nm is expected due to the tolerances in the fabrication procedure, which has only a small influence on the perceived color (inset of Fig. 6c).

PHEMA can also act as negative tone photoresist when PAG is added in its solution forming the PHEMA-N solution. In this way the thickness of the individual layers could be modulated for both materials adding further flexibility in the design and the desired properties of the photonic crystal array. Substrates having 4 different PCs are also fabricated by employing gray scale lithography in all layers with the procedure illustrated in Fig. 7.

First the PHEMA-N is applied via spin-coating and PAB follows. For the needs of the present work, a 6% w/w solution of PHEMA in EL with 2% w/w PAG on the basis of the amount of polymer was used; spin-coating was accomplished at 7000 rpm and led to a

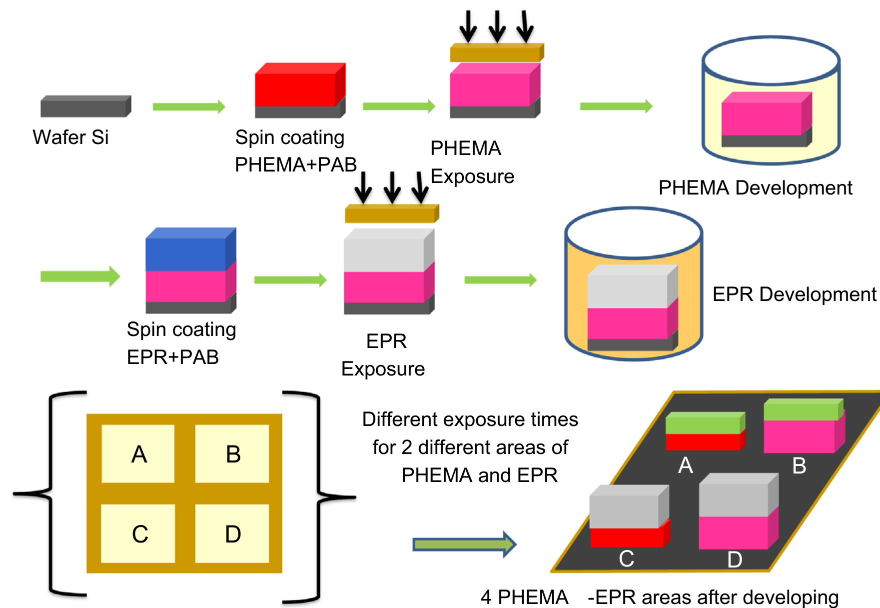

Fig. 7. Schematic presentation of the fabrication of a Cross-PHEMA/Cross-EPR array having 4 different PCs. In this scheme both EPR and PHEMA act as lithographic materials.

Table 2
The exposure dose for each PHEMA and EPR area and the the average thickness of PHEMA and EPR films for each PC of the array.

	PHEMA exposure dose (mJ/cm^2)	EPR exposure dose (mJ/cm^2)	Average PHEMA thickness (nm)	Average EPR thickness (nm)
Area A	6	7×10^{-4}	117.4 ± 7.3	72.8 ± 11.0
Area B	8	7×10^{-4}	133.3 ± 7.7	68.4 ± 7.0
Area C	6	10×10^{-4}	110.1 ± 11.1	97.9 ± 10.4
Area D	8	10×10^{-4}	134.6 ± 9.3	89.7 ± 5.0

film thickness of 140 nm while PAB ($T=120$ °C, $t=5$ min) followed. Then the layer was exposed via an appropriate mask at a low dose for two areas and a high dose for another two areas (e.g. area A, C low dose and B, D high dose). PEB was then made at 90 °C for 2 min and the samples were developed in methanol for 1 min. Then the EPR film was spin-coated on top of the patterned PHEMA film and PEB. The EPR solution and baking time were the same as described above. After PAB, two areas of EPR were exposed at low dose and two areas at high dose (area A, B low dose and area C, D high dose), followed by PEB and development, giving four areas having different PHEMA and EPR film thicknesses. The same procedure was applied for each of the ten fabricated bilayers. In this way four photonic filters were fabricated on the substrate each one having a different refractive spectra due to the different Cross-EPR and Cross-PHEMA film thicknesses with no material left between the photonic filters (i.e. the unexposed areas of both materials between the PCs). In Table 2 the average thickness of PHEMA and EPR films in each PC is given and in Fig. 8 the layer thickness of each PHEMA and EPR films for areas A and D (both photoresists exposed with low, A, and high exposure dose, D, respectively) are given. Nevertheless the film thickness difference of PHEMA of each PC is no more than 10%. The EPR film thickness difference for each PC is higher mostly at the lower exposure dose areas due to the fact that EPR has lower contrast at this exposure dose range and thus minor exposure dose difference results in different film thicknesses.

The optical properties of the final structures are shown in Fig. 9. The peak reflectance has now increased compared to the previous arrays, where only the thickness of EPR layers were changed mainly because more bilayers are added (10 versus 8). Reflectance peak shifts ranging from 20–50 nm in 4 different regions of the array in fabricated structures were observed. Our analysis (Fig. 9c) shows that the fabrication tolerances in the control of the thickness of the layers are not detrimental in the design of PC arrays with tailored optical properties.

4. Conclusions

In the present work, the fabrication and characterization of 1-D polymeric photonic crystal arrays were presented. The realization of the PC arrays was achieved via conventional lithographic techniques (spin-coating, PAB, DUV exposure, PEB and development), of PHEMA and EPR, which are both negative gray-tone chemically amplified resists when adequate PAG is added to them. The thickness of the resist film after development can be controlled by applying an exposure dose lower than the optimal lithographic dose. PC arrays were fabricated using two alternative approaches. First regions on the substrate were differentiated by keeping constant the PHEMA layer thickness (no PAG added to PHEMA) and varying the EPR thicknesses (different exposure doses). An array of four PCs having distinct reflectance spectra was fabricated using this procedure.

In our second approach both materials were used as lithographic materials. Two areas of the array were exposed at low dose for PHEMA and the other two areas with high dose. The same procedure was followed for EPR except that the low dose EPR area was one above the low and one above the high PHEMA dose and the same was true for the high exposure dose of EPR. In this way, an array of four different PCs having different reflectance spectra was fabricated.

The tuning range of the position of the peak reflectivity can be further enhanced by employing layers with larger thickness range i.e. from few tens of nanometers to few hundred of nanometers. The concept introduced in this work is the tunability within the visible range and for that reason the layer thicknesses employed were selected to provide the reflectance peak in this range. The on/off ratio in the reflectance curve could be further increased by increasing the number of bilayers. Furthermore the use of gray scale lithography

a

Cross-PHEMA
Cross-EPR
Layer Thickness (nm)
Layer Number

b

Cross-PHEMA
Cross-EPR
Layer Thickness (nm)
Layer Number

c

IMEL SE GB-L SEI 1.0kV X35,000 WD 2.2mm 100nm

d

IMEL SE GB-L SEI 1.0kV X25,000 WD 2.3mm 1μm

Fig. 8. The layer thickness of each PHEMA and EPR film in (a) area A (lower exposure dose for both materials) and (b) area D (highest exposure dose for both materials) and (c and d) the cross-section SEM pictures of those areas respectively.

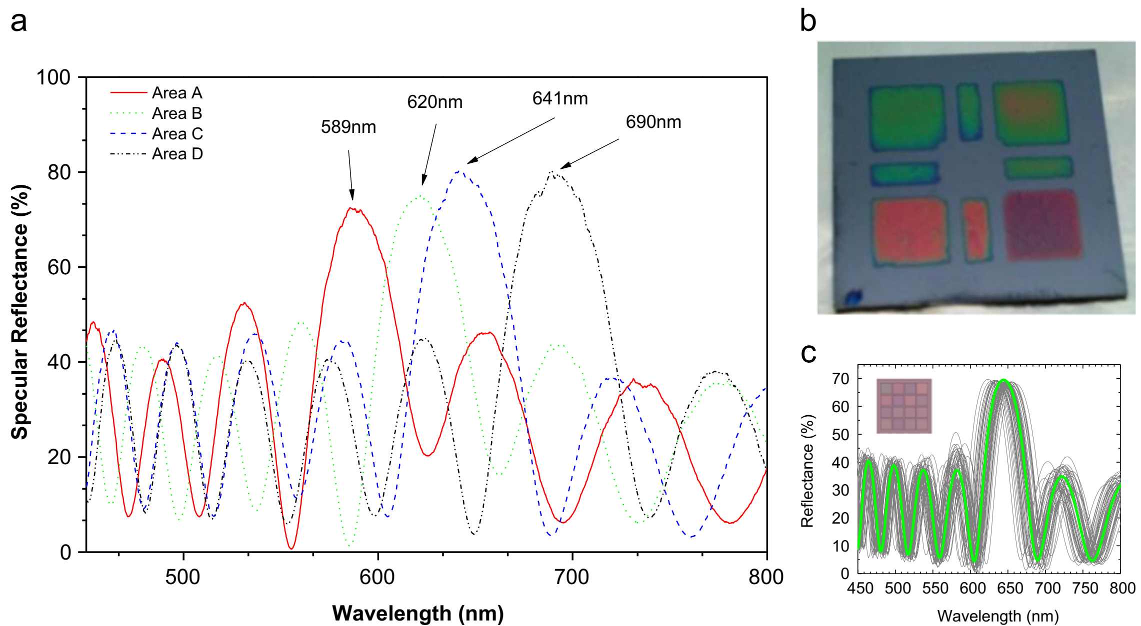

Fig. 9. a The reflectance spectra of each area of the PC array fabricated with the procedure described in fig. 7 and (b) an optical image of the array. (c) Numerical calculation of the specular reflectance for random versions of Area C using the thicknesses and standard deviations quoted in Table 1. Fifty different random realizations are shown with gray lines, while the perfect case is shown with the thick green line. In the inset, the theoretical color of 16 different realizations is shown in the small squares, while the perfect case is shown in the large background square. (For interpretation of the references to color in this figure legend, the reader is referred to the web version of this article.)

allows for the realization of higher number of areas with different thicknesses on the same substrate. The number of areas that will have distinguishable reflectance spectra is defined by the particular thickness variation tolerance.

The use of conventional lithographic techniques for the fabrication of PC arrays allows for the choice of the desired spectral regimes of operation, the dimensions (belonging to the micro region), the shape and the exact position of the array in a device, while the possibility to use transparent, or flexible substrates allows for a variety of applications.

Acknowledgments

This work was supported by the research project entitled "Resonant phoTonic-pHononic nanostrUctures for enhanced acoustooptic interaction: phoxoNic DEvice Realization (THUNDER)" co-financed by the European Union (European Regional Development Fund – ERDF) and Greek National Funds.

References

[1] Gondek E, Karasinski P. One-dimensional photonic crystals as selective back reflectors. Opt. Laser Technol 2013;48:438–46.
[2] González-García L, Lozano G, Barranco A, Míguez. H, González-Elipe AR. TiO_2–SiO_2 one-dimensional photonic crystals of controlled porosity by glancing angle physical vapour deposition. J Mater Chem 2010;20:6408–12.
[3] Choi SY, Mamak M, Von Freymann G, Chopra N, Ozin G. A Mesoporous bragg stack color tunable sensors. G Nano Lett. 2006;6:2456–61.
[4] Mao L, Ye H. New development of one-dimensional Si/SiO_2 photonic crystals filter for thermophotovoltaic applications. Renew Energy 2010;35:249–56.
[5] Lazarova K, Awala H, Thomas S, Vasileva M, Mintova S, Babeva T. Vapor responsive one-dimensional photonic crystals from zeolite nanoparticles and metal oxide films for optical sensing. Sensors 2014;14:12207–18.
[6] Bailey J, Sharp JS. Thin film polymer photonics: spin cast distributed bragg reflectors and chirped polymer structures. Eur Phys J E 2010;33:41–9.
[7] Edrington AC, Urbas AM, DeRege P, Chen CX, Swager TM, Hadjichristidis N, et al. Polymer-based photonic crystals. Adv Mater 2001;13:421–5.
[8] Yagi R, Katae H, Kuwahara Y, Kim S-N, Ogata T, Kurihara S. Polymer 2014;55:1120–7.
[9] Georgaki M-I, Botsialas A, Argitis P, Papanikolaou N, Oikonomou P, Raptis I, et al. 1-D polymeric photonic crystals as spectroscopic zero-power humidity sensors. Microelectron Eng 2014;115:55–60.
[10] Wang Z, Zhang J, Li J, Xie J, Li Y, Liang S, et al. Colorful detection of organic solvents based on responsive organic/inorganic hybrid one-dimensional photonic crystals. J Mater Chem 2011;21:1264–70.
[11] Kitsara M, Goustouridis D, Chatzandroulis S, Chatzichristidi M, Raptis I, Ganetsos TH, et al. Single chip interdigitated electrode capacitive chemical sensor arrays. Sens Act B 2007;127:186–92.
[12] Vasilopoulou M, Boyatzis S, Raptis I, Dimotikalli D, Argitis P. Evaluation of poly (hydroxyethyl methacrylate) imaging chemistries for micropatterning applications. J Mater Chem 2004;14:3312.
[13] Argitis P, Raptis I, Aidinis CJ, Glezos N, Baciocchi M, Everett J, et al. An advanced epoxy novolac resist for fast high resolution e-beam lithography. JVac Sci Technol B 1995;13:3030–4.
[14] Chatzichristidi M, Raptis I, Argitis P, Everett J. Partially hydrogenated poly (vinyl phenol) based photoresist for near UV, high aspect ratio micromachining. J Vac Sci Technol B 2002;20:2968–72.
[15] Stewart KJ, Hatzakis M, Shaw JM, Seeger DE, Neumann E. Simple negative resist fro deep ultraviolet, electron beam and X-ray lithography. J Vac Sci Technol B 1989;7:1734–9.
[16] Moreau WM. Semiconductor Lithography: Principles, Practices, and Materials. Springer, UK: Basic Books; 1988.